Supporting Information

Epitaxial Transfer through End-Group Coordination Modulates Odd-Even Effect in Alkanethiol Monolayer Assembly

Yeneneh Y. Yimer[‡a], Kshitij C. Jha[‡a], and Mesfin Tsige*[a]

[a]Department of Polymer Science, The University of Akron, Akron, OH 44325
* Corresponding author: mtsige@uakron.edu
‡These authors contributed equally to this work

S1. Models, Parameters and Protocols of MD Simulation

Models and Parameters

All-atom molecular dynamic simulations were carried out to study self assembly of n-alkanethiol monolayers on Au {111} surface. Two systems of hydroxyl and methyl end terminated n-lkanethiols with different chain lengths (n=11-32) are considered. Accurate and optimized potential for gold {111}[26] were utilized, which have been shown to reproduce properties for metals at biological and aqueous interafces in good agreement with experiment, including surface freezing, adsorption energies, specific adsorption on facets and orientation of water.[26,29,31,S1-S3] The force field parameters for *n*-alkanethiols were obtained from the optimized potential for liquid simulations-all atom (OPLS-AA)[27] that have been optimized for both alkanes and *n*-alkanethiols[S4] and extensively used for studying properties of monolayer assembly.[S5,S6]

The Au {111} surface with a cross sectional area of ~ 6x6 nm^2 (60.499x59.856 $Å^2$) and vertical thickness of ~ 3 nm (28.256 Å) was constructed using metal unit cell with parameters obtained from x-ray data[S7] using the graphical interface of Materials Studio 6.0. [S8] A total of 6096 atoms were part of the gold {111} surface in the simulation. We choose 6x6 nm^2 as it has been previously reported that 6 nm is the minimum size of the gold surface for relatively defect free assembly of monolayers.[S9]Additionally, systems with ~12x12 nm^2 were also analyzed for all systems, but no appreciable difference in monolayer assembly characteristics was observed. To retain computational efficiency, ~ 6x6 nm^2 system sizes were used for all analyses.

The van der Waals interactions for the system are described by the 12-6 Lennard-Jones potential (LJ). The interaction parameters (σ_{ij} and ε_{ij}) for the hetero-atomic (including between alkanethiol and Au) interactions are specified by the geometric mean of the homo-atomic parameters for both *n*-alkanethiols and Au, as is the case with the OPLS-AA force field. For intra-molecular interactions between atoms separated by three bonds,

the interaction potential is reduced by a factor of 2, following the OPLS-AA force field paradigm.

Protocols

The sulfur atoms of SH-$(CH_2)_n$-OH/ SH-$(CH_2)_n$-CH_3, with n varied from 11-32 were initially placed at 3 Å above the top Au layer with ($\sqrt{3}$ $X\sqrt{3}$) R30° triangular lattice as reported in literature[21] with lattice constant a = 4.995 Å. The *n*-alkanethiols initially orient normal to the Au surface. The total numbers of alkanethiol chains in the system are 168 with surface coverage of 21.55 $Å^2$ per chain for a coverage density of ~5 chains/nm^2. All the simulation was carried out in the NVT ensemble. The initial equilibration was done by heating the system from 20 K to 300 K with discrete steps of 20 K/50 ps. After the equilibration, the systems were run at a temperature of 300 K for additional 5 ns.

Dynamics of transfer, monolayer stability, and variance in distributions (adatom profile and tilt angle) were analyzed by heating equilibrated systems from 300 K to 400 K followed by cooling from 400 K to 300 K in discrete steps of 10 K/ 200 ps. For accurate analyses at each temperature, the last snapshot from the heating cycles were run for more than 2 ns and data collected in the equilibrated phase as seen through block averages of total energy.

All simulations were carried out using the LAMMPS simulation package.[S9] The equations of motion were integrated using the velocity-Verlet algorithm using a time step of 1 fs. For NVT ensembles, a Nosé-Hoover thermostat with a damping time of 100 fs was used to maintain the temperature of the system. For the non-bonded interactions, the cutoff radius was fixed at 12 Å and the long-range Coulomb interactions (beyond the cutoff radius) were calculated using the particle-particle/particle-mesh(PPPM) algorithm.[S10]

S2. Tilt Angle Computation

The tilt angle θ is the angle between the z axis, viz. normal to the gold surface, and a vector used to describe the orientation of different parts of *n*-alkanethiols. For hydroxyl terminated we define two orientation vectors. The first vector (also referred to as S-O tilt angle) goes from sulfur atom of the thiol group to the oxygen atom on the hydroxyl group, as shown in Figure 1A. The second vector (also known as the S-C tilt angle) goes from the sulfur atom of the thiol group to the carbon atom of the methylene group dierctly bonded to the end terminal hydroxyl group as shown in Figure 1B. For methyl terminated *n*-alkanethiols the orientation vector is defined as the vector going from the sulfur atom of the thiol to the carbon atom in the methyl group as shown in Figure 1C. Figure S1 shows variation in tilt angle for methyl terminated *n*-alkanethiols, and the chain length dependence on peak is similar to that of hydroxyl terminated *n*-alkanethiols (S-C tilt angle distribution shown in Figure 3). The temperature dependent S-C tilt angle profile for hydroxyl terminated *n*-alkanethiols (Figure S2) also shows a systematic shift

to the left (or lower tilt angle) as observed for S-O tilt angle distribution temperature dependence in Figure 4B.

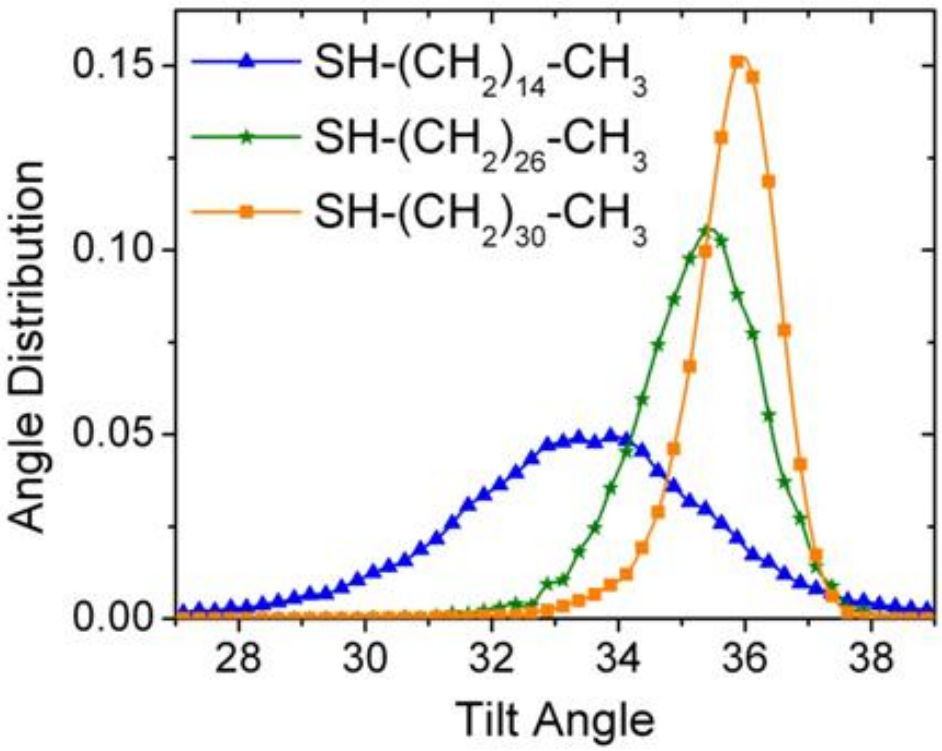

Figure S1. Tilt angle distribution at 300 K for three chain lengths (n=14, 26, 30) for methyl-terminated *n*-alkanethiols.

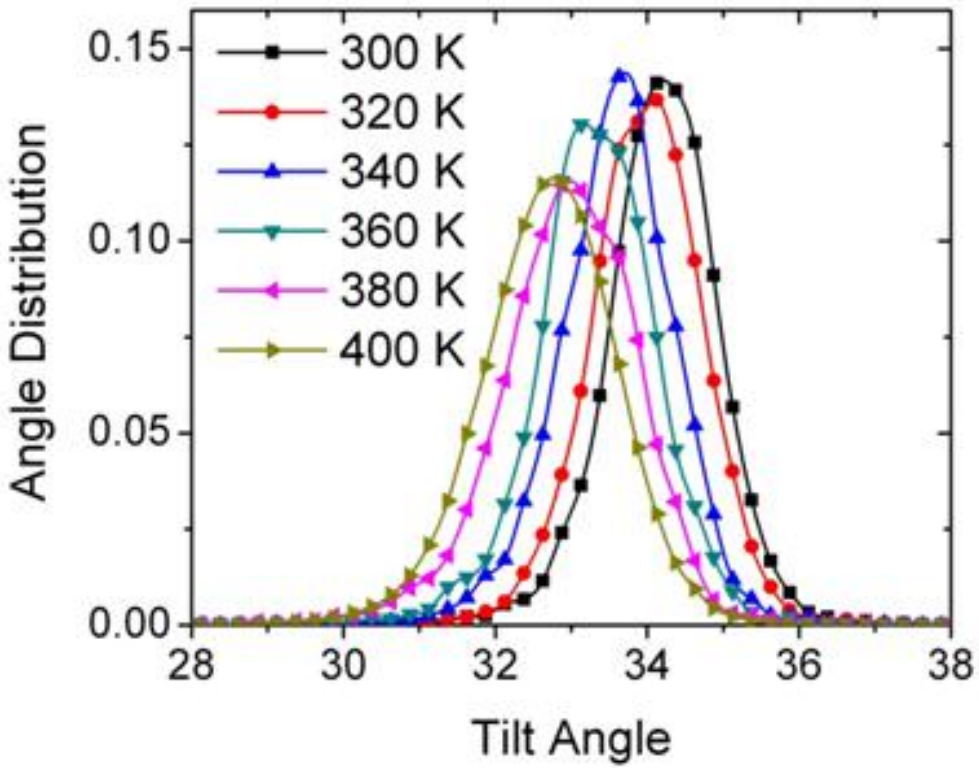

Figure S2. S-C tilt angle distribution for hydroxyl-terminated alkanethiol (n=30) from 300 to 400 K.

S3. Hydrogen Bond Computation

For hydroxyl-terminated *n*-alkanethiols hydrogen bond is computed by setting the following geometrical criteria: oxygen-oxygen distance ≤ 3.5 Å, oxygen-hydrogen distance ≤ 2.5 Å and O-H--O angle≥120° per assignments in literature[S11,S12,34] adjusted to the present two dimensional hydrogen bonded network. At each time step, the number of hydrogen bonds are computed and averaged over a minimum of 100 snapshots. In Figure S3 we see the distribution plot for hydroxyl terminated (n=30) alkanethiol at 300 K.

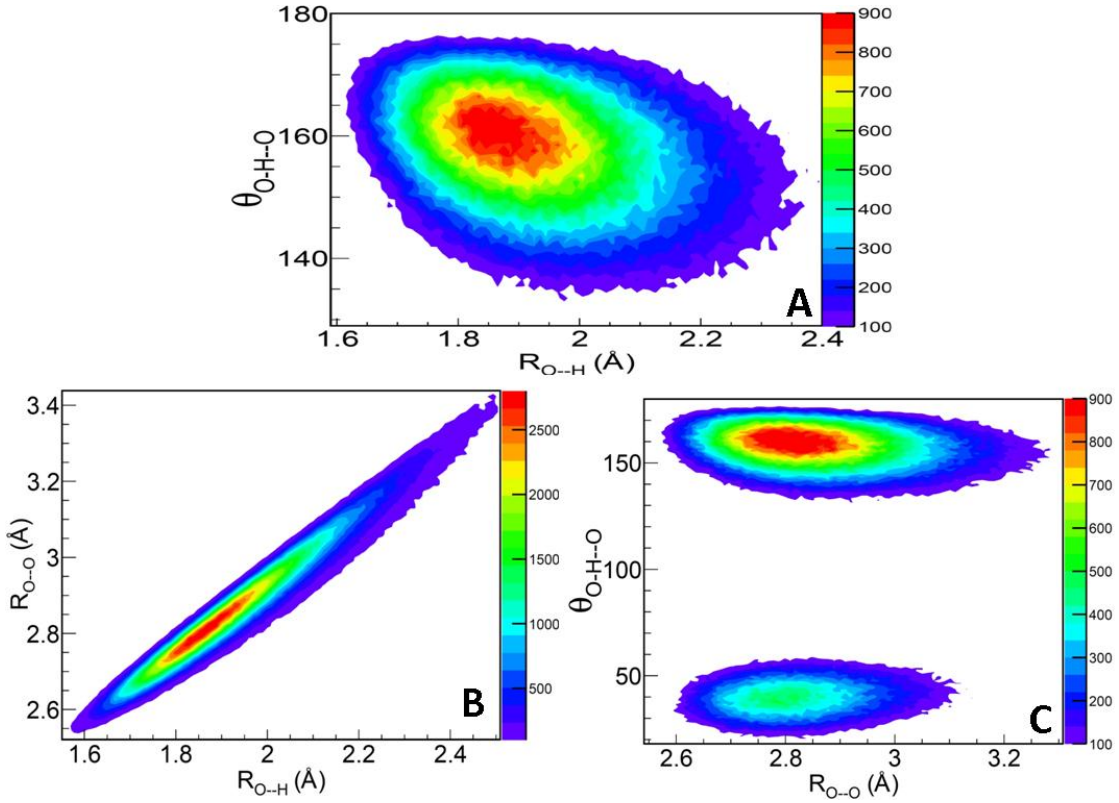

Figure S3. Distribution plots of hydrogen bonded network for SH-$(CH_2)_{30}$-OH at 300 K. The distribution plots are a) Hydrogen bond angle (of oxygen-hydrogen---oxygen) vs the hydrogen bond distance (oxygen---hydrogen). b) The distance between neighbor oxygens participating in hydrogen bonding versus the distance between oxygen and hydrogen participating in the hydrogen bonding. c) The angle (oxygen-hydrogen---oxygen) vs. distance between neighbor oxygens participating in hydrogen bonding. All counts are cumulative over 800 snapshots.

S4. Adatom Computation

The adsorption sites of sulfur on Au {111} were categorized into three major groups: atop, bridge and hollow, shown in Figure S4. Atop is when the sulfur atom is on top of first layer of Au, Bridge is midway between two Au atoms of the top layer and Hollow is when the sulfur is on the top of either second layer (HCP) or third layer (FCC) of Au. To take into account the dynamic nature of the adsorption sites we categorize them based on the closest sulfur-gold distance (projection on the x-y plane). The percentages of adsorption sites for different system are shown in Tables S1 and S2.

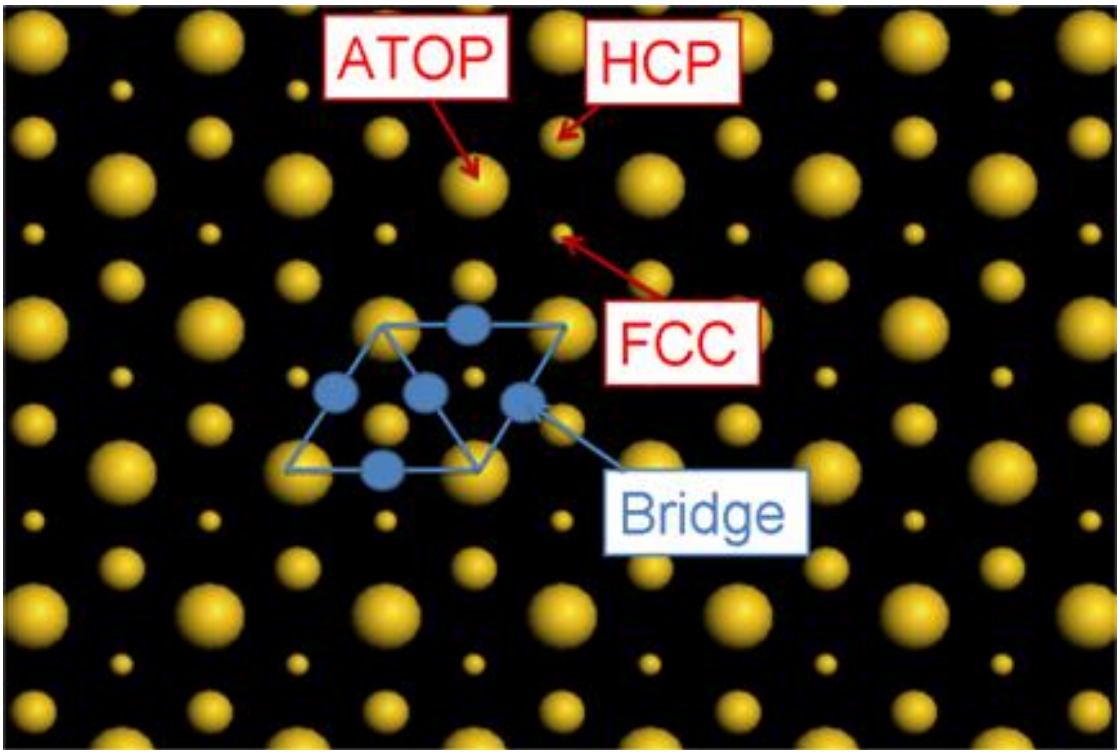

Figure S4. Schematic for different adsorption sites for S of n-alkanethiol on Au {111}. Only the gold surface is shown. Three layers of gold are shown with decreasing radii of the spheres. The bridge, atop, hcp, and fcc sites are shown. A unit lattice is marked in blue to illustrate the bridge adsorption site.

Energy per sulfur (adsorption energy) is computed by calculating non bond (coulomb and LJ) interaction energy of sulfur with all atoms of *n*-alkanethiols and gold that would take into account the packing of the monolayer at a given state for a given adsorption site. This interaction non bond energy can be seen as a sum of three parts and gives a comprehensive view of how energetically favorable the adsorption at a given site is:

$$E_{Sulfur} = E_{Au\text{-}Sulfur} + E_{Sulfur\text{-}Sulfur} + E_{Sulfur\text{-}Monolayer}$$

(Surface interaction) (Self interaction) (Monolayer interaction)

This was averaged for all adsorption sites of a give type (hollow, bridge, atop) available in the trajectory. Error for the computation was estimated as ±0.01 kcal/mol for averaging over ~100 snapshots.

Table S1. Adsorption energy per site for hydroxyl terminated n-alkanethiol as a function of chain length. All values are in kcal/mol.

Spacer Length	Atop	Bridge	Hollow
14	-3.08	-3.41	-3.48
20	-3.10	-3.41	-3.48
26	-3.09	-3.41	-3.48
30	-3.11	-3.42	-3.47

Table S2. Adsorption energy per site for methyl terminated n-alkanethiol as a function of chain length. All values are in kcal/mol.

Spacer Length	Atop	Bridge	Hollow
14	-3.12	-3.41	-3.48
20	-3.10	-3.42	-3.48
26	-3.09	-3.40	-3.47
30	-2.31	-3.39	-3.45

Table S3. Adsorption site percentage for hydroxyl terminated *n*-alkanethiols as a function of chain length and temperature.

n	Temperature(K)	System	Atop	Bridge	Hollow
14	**300**	Initial equilibrated	3.18 ±0.22	50.55 ±0.69	46.27 ±0.73
14	**400**	Step heated	4.54 ±0.10	52.67 ±0.26	42.79 ±0.26
14	**300**	Step cooled	3.90 ±0.12	50.94 ±0.38	45.16 ±0.38
20	**300**	Initial equilibrated	3.42 ±0.08	50.62 ±0.27	45.96 ±0.26
20	**400**	Step heated	4.70± 0.16	53.74 ±0.35	41.56 ±0.34
20	**300**	Step cooled	3.47± 0.11	50.97 ±0.35	45.56±0.34
26	**300**	Initial equilibrated	2.43 ±0.07	52.29 ±0.24	45.28 ±0.23
26	**400**	Step heated	4.52±0.15	53.74 ±0.38	41.74 ±0.36
26	**300**	Step cooled	1.83±0.07	51.17 ±0.31	47.00 ±0.32

Table S4. Adsorption site percentage for methyl terminated *n*-alkanethiols as a function of chain length and temperature.

n	Temperature(K)	System	Atop	Bridge	Hollow
14	**300**	Initial equilibrated	2.29 ± 0.13	46.68± 0.44	51.03± 0.43
14	**360**	Step heated	4.74± 0.19	51.73 ± 0.44	43.53±0.43
30	**300**	Initial equilibrated	1.64± 0.07	55.62± 0.27	42.74 ± 0.27
30	**400**	Step heated	2.53± 0.13	56.43± 0.34	41.04 ±0.35

S5. Epitaxial Transfer Computation

The radial distribution of the sulfur atom of the thiol group for both hydroxyl and methyl terminated *n*-alkanethiols (Figures S5B, D and S6B), the oxygen atom of the hydroxyl group for hydroxyl terminated *n*-alkanethiols (S5A, C), carbon of the methyl group (S6A) for methyl terminated *n*-alkanethiols are computed for different chain lengths and

temperatures. For each chain length and temperature, the variance in first peak of the radial distribution is calculated signifying the variance in the nearest neighbor distance. The epitaxial transfer for each chain length is quantified by taking the rate of change of the variance of the first peak of radial distribution of O of hydroxyl or C of methyl group with respect to variance of the first peak of radial distribution of the sulfur atom at different temperatures (Figure S7).

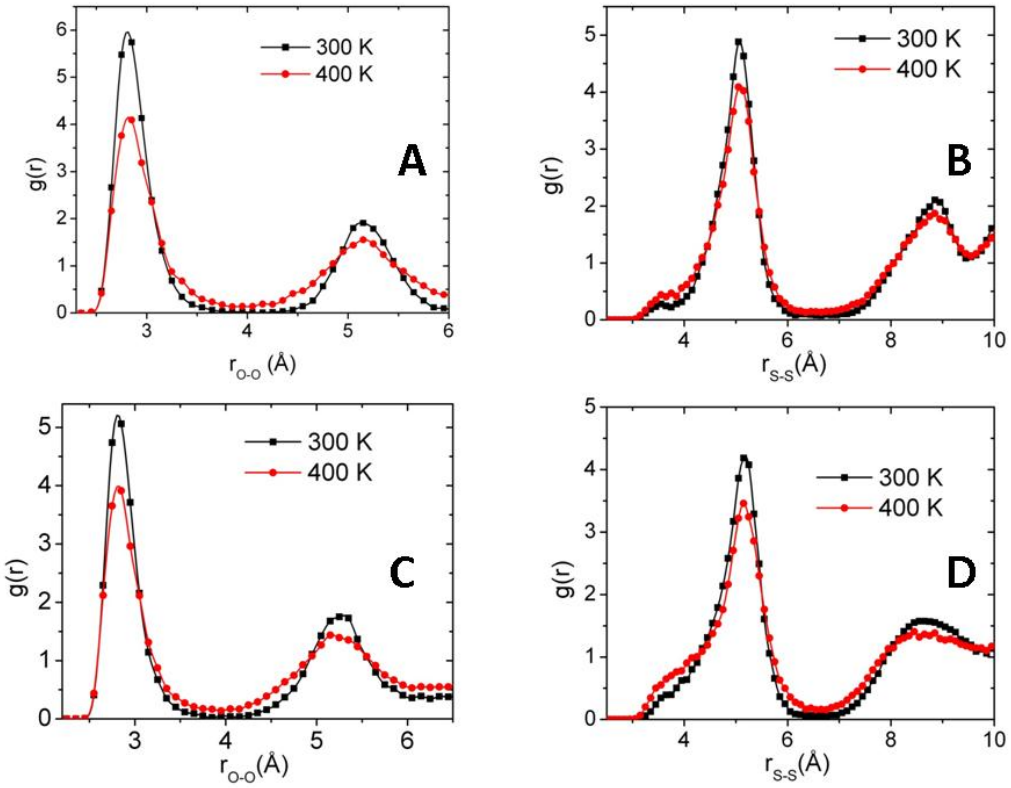

Figure S5. Radial distribution (g(r)) for hydroxyl-terminated *n*-alkanethiols at 300 K and 400 K. A) g(r) of O-O for hydroxyl terminated n-alkanethiol (n=14). B) g(r) of S-S for hydroxyl terminated n-alkanethiol (n=14). C) g(r) of O-O for hydroxyl terminated n-alkanethiol (n=30). D) g(r) of S-S for hydroxyl terminated n-alkanethiol (n=30). For all cases, variance in first peak is considered for computation of epitaxial transfer.

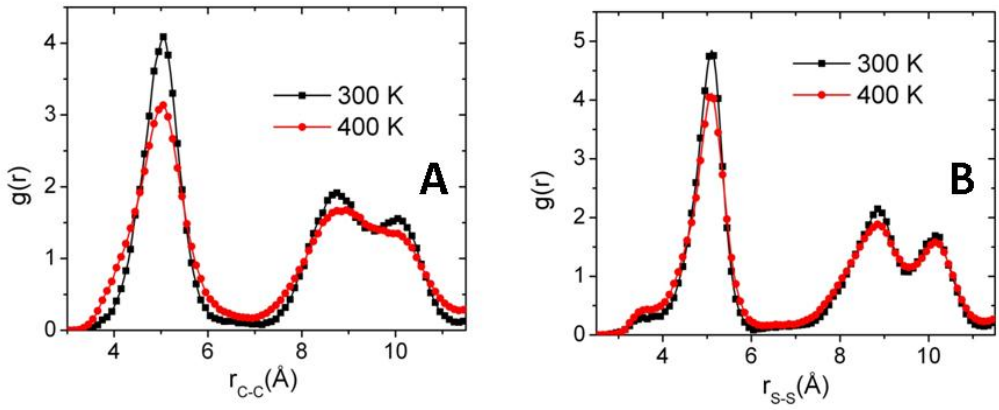

Figure S6. Radial distribution (g(r)) for methyl-terminated *n*-alkanethiols at 300 K and 400 K. A) g(r) of C-C for mehtyl terminated n-alkanethiol (n=30). B) g(r) of S-S for mehtyl terminated n-alkanethiol (n=30).

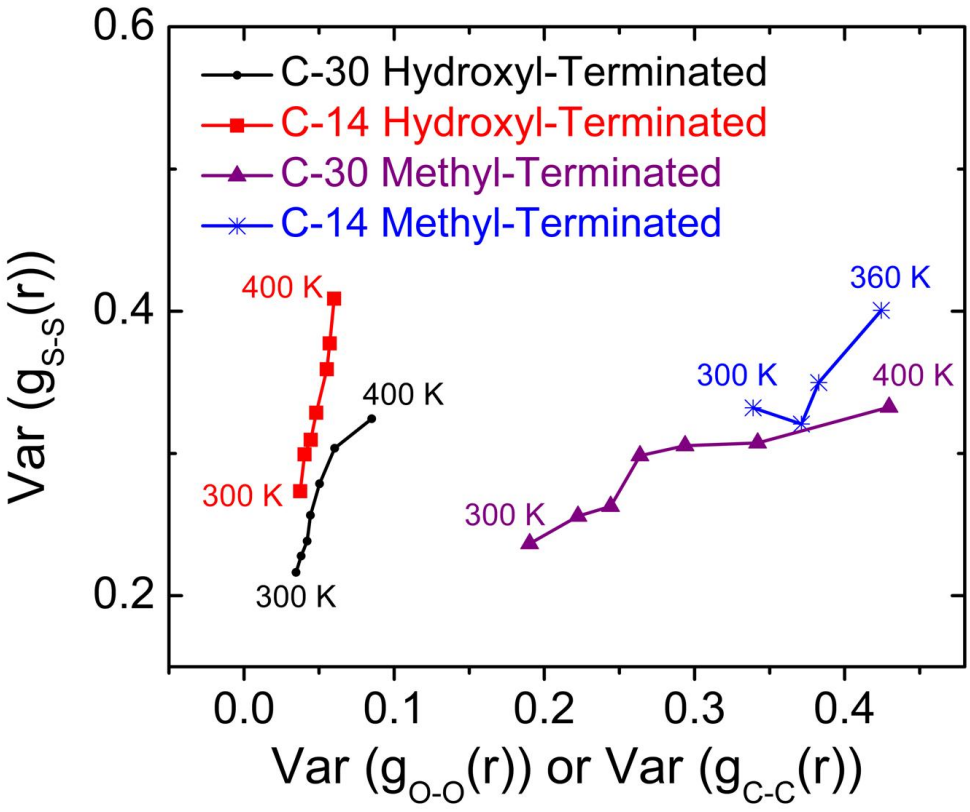

Figure S7. Epitaxial transfer shown for hydroxyl terminated (n=14,30) and methyl terminated (n=14,30) *n*-alkanethiols. The monolayers lose stability after 400K for n=30 hydroxyl and methyl terminated, n=14 hydroxyl terminated and 360K for n= 14 methyl terminated. These instabilities are shown by spikes for two cases (n=30, hydroxyl and n=14, methyl terminated *n*-alkanethiols).

S6. Energy per Chain Computation

The energy per chain is computed by summing the total non-bonded energy (LJ + Coulomb) between *n*-alkanethiols (both inter-chain and intra-chain) with the interaction energy between Au and alkanethiol and then dividing the sum by the total number of n-alkanethiol chains (168 in this case). Figure S8 shows the chain length dependence of energy per chain for both hydroxyl and methyl terminated *n*-alkanethiols. For both cases, hydroxyl and methyl terminated, the energy per chain decreases with increase in chain length (Figure S8A,B, D) mainly due to LJ interactions (Figure S8B) which stabilize the packing of the monolayers. Moreover, the total energy per chain for hydroxyl terminated monolayers is lower than the methyl terminated monolayers due to stability provided by hydrogen bonded top network which is mainly provided by the coulomb stabilization (Figure S8C).

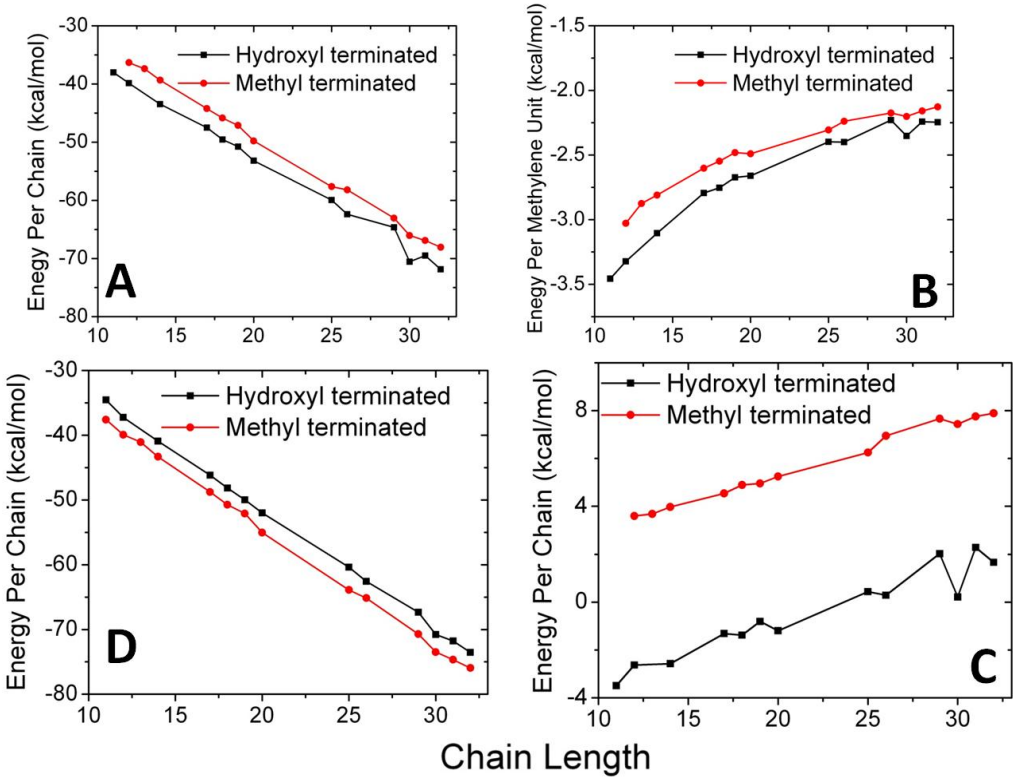

Figure S8. Energy per chain for hydroxyl and methyl-terminated *n*-alkanethiols at 300K. A) Total non-bond energy (LJ + Coulomb). B) Total non-bond energy (LJ + Coulomb) per methylene unit. C) Coulomb interaction energy. D) LJ potential. Maximum error is ±0.013 kcal/mol.

S7. Chain Mobility Computation

To quantify the n-alkanethiol chain mobility we calculate the average (over all 168 chains in the system) root mean square displacement (RMSD) of sulfur atom of the thiol group as a function of time, as shown in Figure S9. By fitting the plateau region of RMSD, which represents the equilibrated state of the system, to a constant we obtained the root mean square displacement for a given chain length.

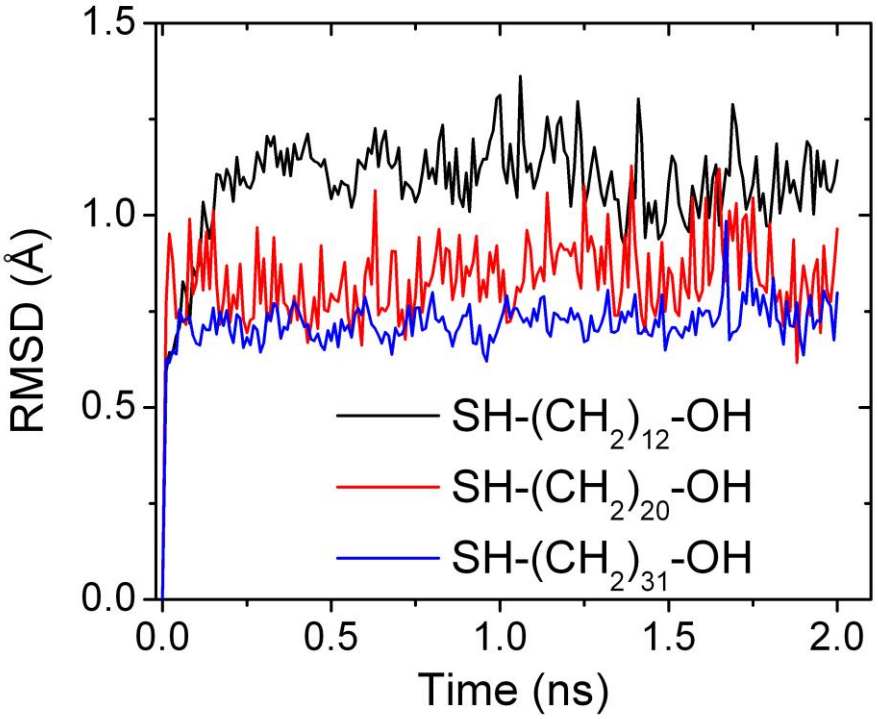

Figure S9. Root mean square displacement as a function of time of hydroxyl-terminated *n*-alkanethiols for three different chain length (n = 12, 20 and 31) at 300 K. The distribution is after an initial equilibration of 3 ns at the same temperature.

References

S1. H. Heinz, B. L. Farmer, R. B. Pandey, J. M. Slocik, S. S. Patnaik, R. Pachter and R. R. Naik, *J. Am. Chem. Soc.***2009**, 131, 9704.

S2. H. Heinz, K. C. Jha, J. Luettmer-Strathmann, B. L. Farmer and R. R. Naik, *J. R. Soc. Interf.* **2011**, 8, 220.

S3. R. Coppage, J. M. Slocik, B. D. Briggs, A. I. Frenkel, H. Heinz, R. R. Naik and M. R. Knecht, *J. Am. Chem. Soc.* **2011**,133, 12346.

S4. W. L. Jorgensen, D. S. Maxwell and J. Tirado-Rives, *J. Am. Chem. Soc.* **1996**, 118 11225.

S5. D. Y. Lee, M. M. Jobbins, A. R. Gans and S. A. Kandel, *Phys. Chem. Chem. Phys.* **2013,** 15, 18844.

S6. J. M. D. Lane, M. Chandross, M. J. Stevens and G. S. Grest, *Langmuir* **2008**, 24, 5209.
S7. *CRC Handbook of Chemistry and Physics*, 89th ed.; D. R. Lide, Ed.; CRC press: Boca Raton, 2008.

S8. *Materials Studio 4.0*, *Cerius*^{2}, and *Discover* programs; Accelrys, Inc., San Diego, 2006

S9. T. Djebaili, J. Richardi, S. Abel and M. Marchi, *J. Phys. Chem. C* **2013**, 117, 17791.

S9. S. Plimpton, *J. Comp. Phys.* **1995**,117, 1.

S10. R. W. Hockney and J. W. Eastwood, Computer *Simulation Using Particles* Adam Hilger, Bristol, Philadelphia, **1988**

S11. A. Luzar and D. Chandler, *Phys. Rev. Lett.* **1996**, 76, 928.

S12. A Luzar and D. Chandler, *Nature* **1996**, 379, 55.